CAV2021
11th International Symposium on Cavitation
May 10-13, 2021, Daejon, Korea

The Intensity and Topology Transition of Sheet/Cloud Cavitation at Elevated Temperatures

Mingming Ge[1*], Guangjian Zhang[2], Dhruv Apte[1] and Olivier Coutier-Delgosha[1, 2, *]

[1]Kevin T. Crofton Department of Aerospace and Ocean Engineering, Virginia Tech, Blacksburg, VA 24060, USA
[2]Univ. Lille, CNRS, ONERA, Arts et Metiers ParisTech, Centrale Lille, FRE 2017 - LMFL -Laboratoire de Mecanique des fluides de Lille - Kampe de Feriet, F-59000 Lille, France

Abstract: The effects of temperature on hydrodynamic cavitation in water is investigated in a small-scale Venturi test section. The free-stream conditions are varied with 4 different flow rates and a wide range of temperatures between 28℃ to 63℃. The high-speed visualization and Particle image velocimetry (PIV) system was used to record the cavitating flow and measure the time-resolved velocity field through image post-processing. Results have shown that the cavitation length and sheet/cloud shedding behaviors are influenced by a combination of the pressure drop (indicated with cavitation number σ, the Reynolds' effect (indicated with Reynolds' number Re and the thermal effect (indicated with Thermodynamic parameter Σ). With the temperature increasing, both the cavitation length and thickness experience a 'first growing then suppressed trend'. The cavitation intensity peaks at a transition temperature of 58℃. With the increasing of cavitation length and thickness, the shedding type tends to be transformed from the attached sheet cavity to the detached cloud cavity, and the shedding frequency is decreased correspondingly. In the second stage, the cavitating flow structures are illustrated through Proper Order Decomposition (POD) analysis. Results show that the re-entrant jet (mode 1) and large rotating vortex at the closure (mode2) occupy most of the energy of dynamic behavior of sheet/cloud cavity. The present results allowed us to conduct a qualitative phenomenological analysis of the instability and size evolution of partial cavities by considering thermodynamic effects. And with considering thermodynamic effects, it can be possible to control the cavitation regime by avoiding the peak temperature of transition and reducing the cavity length.

Keywords: Hot water cavitation, Thermodynamic effects, Cavitation dynamics, POD analysis

1. Introduction

Cavitation is a phenomenon in which rapid changes of pressure in a liquid lead to the formation of small vapor-filled cavities or bubbles. The physical process of cavitation can be compared with boiling in which the evaporation occurs when the local temperature of the liquid reaches the saturation temperature (e.g. 100°C at 1 atmospheric pressure). While cavitating vapor appears even at room temperature when the local pressure falls sufficiently far below the saturated vapor pressure (e.g. 0.023 atm for 20°C). Cavitation is a significant cause of wear in some engineering contexts, such as the erosion damage of aircraft propellers, and system vibration of high-speed marine vessels. However, by controlling the flow of the cavitation, the power can be harnessed and non-destructive. For example, it is used to enhance chemical reactions in medicine processing or to eliminate bacteria in the water treatment industry [1, 2].

In most engineering cases the issues with cavitation are related to the hydrodynamic cavitation, dealing with hot water or cryogenic fluids. In contrast to cold water, specific thermodynamic properties considering heat transfer phenomena cannot be negligible. During the bubble growth, the vaporization process requires the latent heat to be supplied by the liquid to the interface. The temperature near the

* Corresponding Author: Olivier Coutier-Delgosha, ocoutier@vt.edu

cavitating region is generally a few degrees below the liquid bulk temperature. This phenomenon leads to a delay in the development of cavitation and a regular decrease in the breakdown cavitation number with increasing temperature, known as the thermodynamic effect of cavitation [3].

Many experimental studies have been dedicated to this thermal delay phenomenon using diverse liquids from water to refrigerants and liquid cryogens. Petkovšek and Dular [4] measured a high-resolution temperature distribution around the cavity for the high-temperature water by a high-speed IR thermography. Dular [5] subsequently studied the erosion of cavitation in the water at 30 °C to 100 °C. He pointed out that the water temperature significantly affected the cavitation aggressiveness. The maximum aggressiveness of cavitation erosion was at around 60 °C.

Although the thermal delay phenomena are widely observed, the reported transition temperature where the thermal effect starts to be significant has not reached a universal consensus. Even for the most investigated pure water, the peak of cavitation length or the maximum cavitation corrosion appears from 40 °C to 70 °C [6-8]. In this experiment, the cavitation is generated in a 3D-printed venturi-type flow channel, with a heating and cooling functioned loop to precisely adjust the water temperature. A high-speed visualization system was used to record the cavitating flow structure, and a PIV (Particle image velocimetry) system was used to measure the velocity field. The image processing and data analysis results show that the methods provided here can obtain a clear observation of the cavitation delay phenomenon due to the so-called thermal effects on cavitation.

2. Experimental Methods

The studied cavitation is generated in a small size Venturi-type test section which is installed in a portable hydraulic loop, as shown in Figure 1a. Two heaters combined with a cooling system are employed enabling the flow temperature to stabilize at a given value which is measured by a thermocouple located upstream of the test section. All of the pipes are thermally protected with vacuum insulation. As shown in Figure 1b, images are recorded with two Fastcam cameras (Photron SA1) positioned on both sides of the Venturi test section. Camera1 on the left side, which is installed with a density filter to reduce the light intensity from particles, could record the light mainly refracted from the vapor phase. Camera2 on the right side, which is installed with a notch filter eliminating the 527nm light refracted from vapor, could record the water phase solely. The location and extent of the instantaneous vapor zones were determined simultaneously with the corresponding water velocity field. The frame rate is 2000 frames/sec while the exposure time is 250us with a frame size of 1024×512 pixels. The time interval between the two laser pulses is 11us. The magnitude of the position change between the particle pairs ranged from 5 to 6 pixels for the given 11us time delay. This corresponds to velocities of 13±0.2 m/s to 16±m/s.

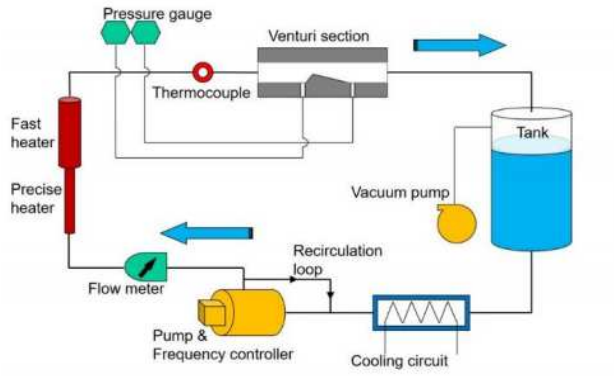

(**a**)

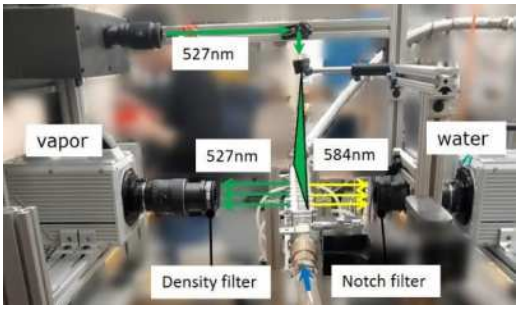

(**b**)

* Corresponding Author: Olivier Coutier-Delgosha, ocoutier@vt.edu

Figure 1. Experimental Setup: (a) hydraulic loop schematic; (b) 2D2C PIV setup.

3. Results and discussions

3.1. Cavitation topology

In this experiment, two kinds of cavity structures can be observed, i.e. the attached sheet cavity and the detached cloud cavity. The attached sheet cavity is characterized by a sheet-shaped cavity that grows from the venturi throat and mainly attaches to the wall. While the detached cloud cavity generates large cavity clouds periodically detaching from the sheet part and vortically shedding away until downstream.

Due to the unsteady behavior of cavitation, the averaged gray level plots are analyzed to get an overall view of all the cases. As shown in Figure 2, from top to bottom, the temperature increased from 28°C to 63 °C. From left to right, the cavitation number decreased from 1.43 to 1.15. Separated by the red dash line, all these 30 cases can be classified into three regimes: the attached cavity type (circled by the single-dot dash line), the cloud cavity regime (circled by the double-dot dash line), and the other 4 transitional cases.

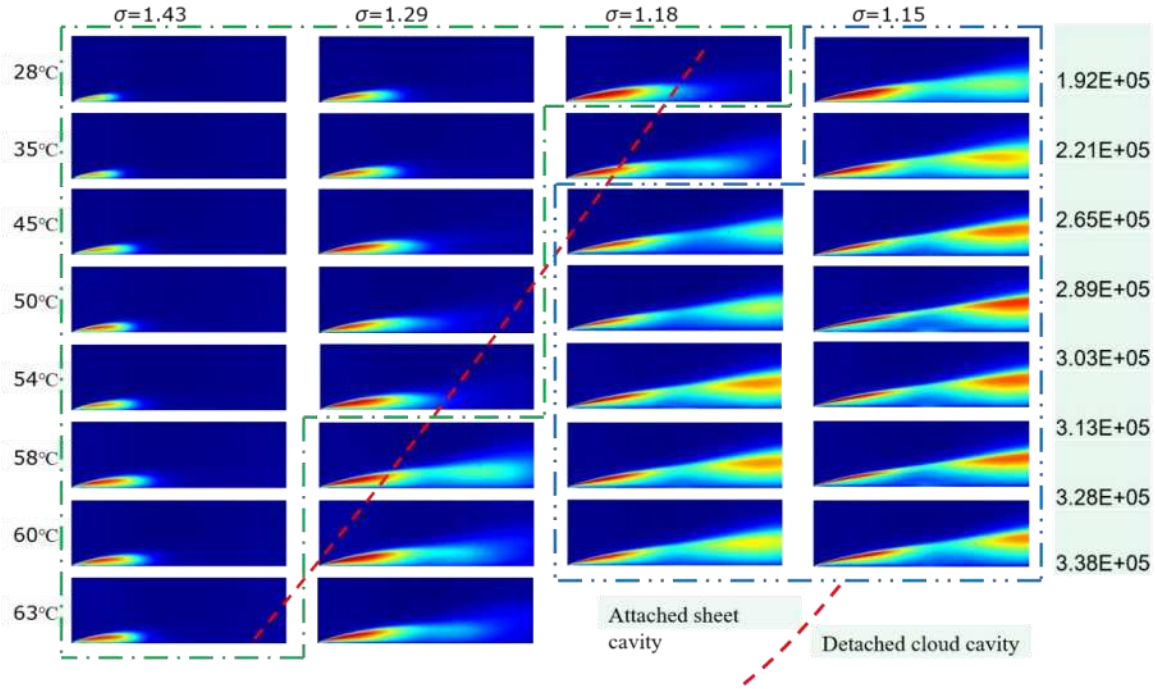

Figure 2. Cavitation topology for cases at different cavitation number and temperatures

3.2. Cavitation length

Besides the flow structure, the temperature change has a strong impact on the extent of cavitation as well. The size denotes the extent of cavitation which can be quantified by the cavity length, thickness, area, or volume in 3D observations. In the present paper, however, we focus on the cavity length determined by the closure region, which is beyond the view for cloud shedding cases 3 and 4. Therefore, the lengths of sheet cavity cases 1 and 2 are calculated and compared, when the cavitation index is high enough that massive cloud shedding does not occur. Figure 3 presents the comparison of cavitation length changing from gray-level images and velocity fields. The thermodynamic effect is visible since for a given cavitation

* Corresponding Author: Olivier Coutier-Delgosha, ocoutier@vt.edu

number, for instance, in case1 σ=1.43 the cavity length decreases with temperature increasing from 58°C to 63°C.

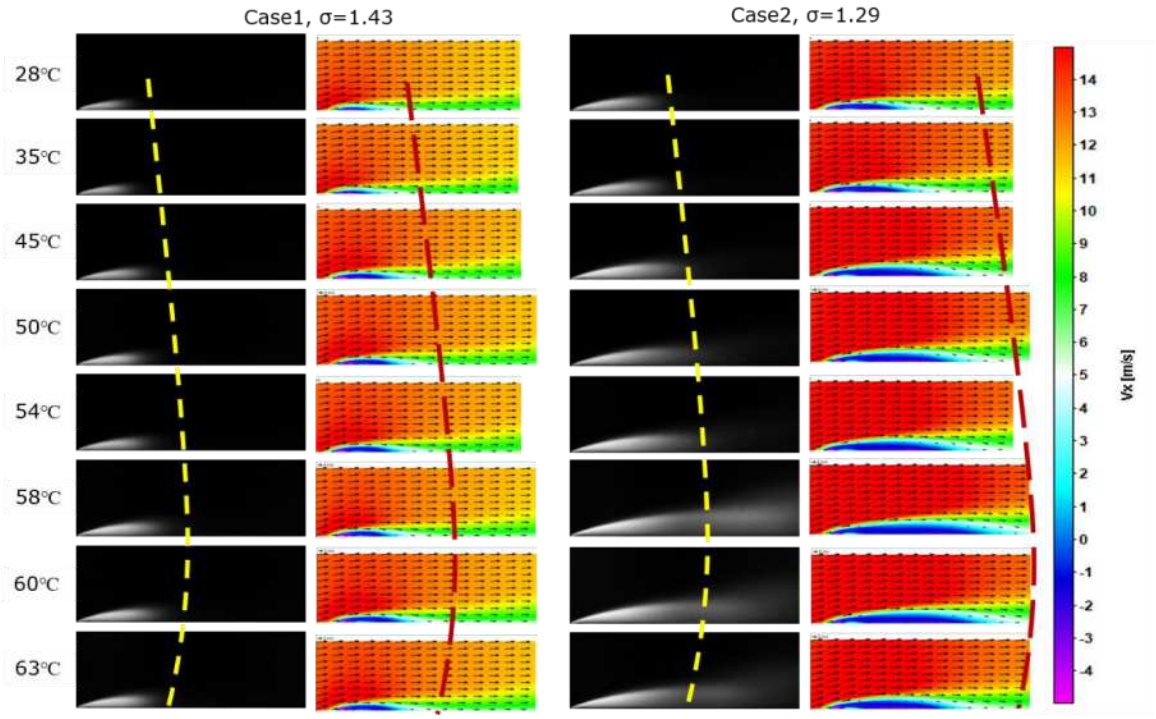

Figure 3. The trend of cavitation length changing as temperature increasing

The explanation is considering that the cavitation generating is affected by two mechanisms, i.e. the viscous effect and the thermal effect. Viscosity decreases with the temperature increasing, and thus Re number increases. As widely accepted in CFD simulation [9] and observed in experiments [10], lower viscosity (i.e. higher Re) had the effect of enhancing cavitation due to weaker molecular bounding. Viscosity explains the increasing trend of cavitation growth of the first part (28°C to 58°C) in Figure 3. However, the thermodynamic effect also needs to be considered that the energy-absorbing during the cavitation process could delays cavitation growth, especially in higher temperatures.

Proposed by Brennen [11], the thermal effect can be quantified by thermodynamic parameter Σ (Eq. (1)):

$$\Sigma = \frac{\rho_v^2 L^2}{\rho_l^2 c_{pl} T_\infty \sqrt{\alpha_l}} \tag{1}$$

As shown in Figure 4, when the temperature is increased, both the Re and nondimensionalized $\Sigma*$ increase. At low temperatures, the thermal effect is not so intense and the cavitation extension is mainly governed by the variation of the Re number. With $\Sigma*$ increasing (over 50 °C) the influence of thermodynamic effects becomes dominant compared with the Reynolds number effect, so the development of the sheet cavity is further weakened or delayed. [8, 12] found that thermodynamic effects become significant from Σ=100 $m/s^{3/2}$ which corresponds to a temperature of 55 °C.

* Corresponding Author: Olivier Coutier-Delgosha, ocoutier@vt.edu

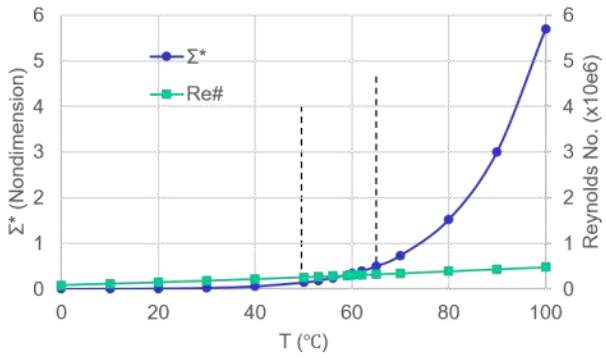

Figure 4. Thermodynamic parameter and Reynolds number changing with temperature

3.3. POD analysis

Figure 5 shows the first two POD modes of the PIV velocity fields of the cavitating flow in case 3 that σ=1.18 at different temperatures. The first two POD modes occupy over 50 percent of the energy for each case. It should be mentioned that at T=28°C, the cavitation type is attached cavity; while at T=58°C, the cavitation type is detached cloud cavity. It can be seen that the first mode represents the re-entrant jet moving upstream, which is the most obvious characteristic for unsteady cavitation. And the second mode represents the large rotating eddy downstream. For the re-entrant jet (mode 1) shown in Figure 5a and 5b, the difference locates in the separation position, i.e., 15mm for the attached cavity, compared with a whole-field recirculation for cloud cavity without separated downstream flow viewed. And for the large rotating eddy (mode 2), the vortexes have a similar shape while the eddy locates earlier for the attached cavity than the cloud cavity.

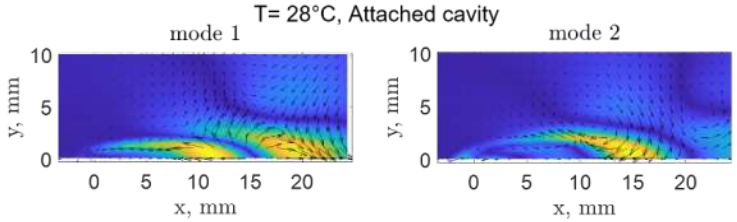

(a)

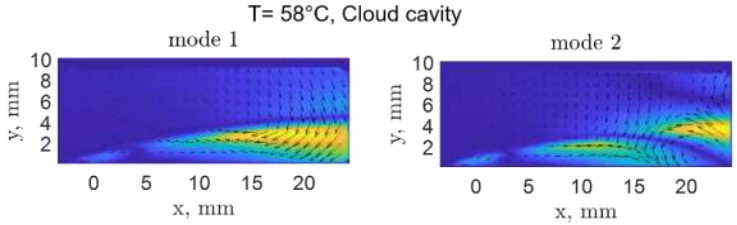

(b)

* Corresponding Author: Olivier Coutier-Delgosha, ocoutier@vt.edu

Figure 4. The first two POD modes of (a) attached cavity and (b) detached cloud cavity.

4. Conclusions

In this study, the unsteady cavitation characteristics and size in different temperatures were investigated. With experiments in 4 cavitation numbers and varying temperatures, the thermal transition temperature is determined at around 58°C. The thermal effect will become dominant beyond that temperature over Reynold's number effect. Additionally, from the POD analysis, the re-entrant jet which triggers the unsteadiness of cloud detachment exists in the first mode and occupies most of the energy in both the attached cavity and cloud cavity.

Acknowledgments: The authors would like to thank this project funded by ONR, under Grant No. N00014-18-S-B001, and the support from Dr. Ki-Han Kim as the ONR proposal manager.

References

1. T. Chen, H. Chen, W. Liu, B. Huang, and G. Wang, Unsteady characteristics of liquid nitrogen cavitating flows in different thermal cavitation mode. Applied Thermal Engineering 2019, 156, 63-76.
2. Zhang L, Zhang G, Ge M, Coutier-Delgosha O. Experimental Study of Pressure and Velocity Fluctuations Induced by Cavitation in a Small Venturi Channel. Energies. 2020 Jan;13(24):6478.
3. J.-P. Franc, G. Boitel, M. Riondet, Ė. Janson, P. Ramina, and C. Rebattet, "Thermody-namic effect on a cavitating inducer—part i: geometrical similarity of leading edge cavitiesand cavitation instabilities," Journal of fluids engineering132(2010).
4. M. Petkov˘sek and M. Dular, "Ir measurements of the thermodynamic effects in cavitatingflow," International Journal of Heat and Fluid Flow44, 756–763 (2013).
5. M. Dular, "Hydrodynamic cavitation damage in water at elevated temperatures," Wear346, 78–86 (2016).
6. Zhang G, Khlifa I, Fezzaa K, Ge M, Coutier-Delgosha O. Experimental investigation of internal two-phase flow structures and dynamics of quasi-stable sheet cavitation by fast synchrotron x-ray imaging. Physics of Fluids. 2020 Nov 1;32(11):113310.
7. H. Zhang, Z. Zuo, K. A. Mørch, and S. Liu, "Thermodynamic effects on venturi cavitationcharacteristics," Physics of Fluids31, 097107 (2019).
8. Petkovsek M, Jacobs D, Ge M, Coutier-Delgosha O. Thermal effects in cavitating flows. APS. 2019 Nov:H02-007.
9. Coutier-Delgosha O, Fortes-Patella R, Reboud JL. Evaluation of the turbulence model influence on the numerical simulations of unsteady cavitation. J. Fluids Eng.. 2003 Jan 1;125(1):38-45.
10. Y. Ito, A. Tsunoda, Y. Kurishita, S. Kitano, T. Nagasaki, Experimental visualization of cryogenic backflow vortex cavitation with thermodynamic effects, Journal of Propulsion and Power 32 (1) (2015) 71–82.
11. Brennen, C., "The dynamic behavior and compliance of a stream of cavitating bubbles," 1973.
12. M. Petkovšek, and M. Dular, Cavitation dynamics in water at elevated temperatures and in liquid nitrogen at an ultrasonic horn tip, Ultrasonics sonochemistry 58 (2019) 104652.

* Corresponding Author: Olivier Coutier-Delgosha, ocoutier@vt.edu